encit 2020

ABCM Associação Brasileira de Engenharia e Ciências Mecânicas

18th Brazilian Congress of Thermal Sciences and Engineering
November 16-20, 2020 (Online)

ENC-2020-0633
Use of Virtual Kinetics Chemistry for Ignition Delay Times Predictions

Augusto Finger Pacheco
Amir Antônio Martins Oliveira
Federal University of Santa Catarina, Florianópolis, SC, Brazil.
augusto.finger@labcet.ufsc.br
amir.oliveira@gmail.com
Benoit Fiorina
Université Paris-Saclay, CentraleSupélec, Laboratoire EM2C, Gif-sur-Yvette, France.
benoit.fiorina@centralesupelec.fr

Abstract. *The simulation of complex reactive flows usually associated with the applications of combustion generally requires a large amount of computational power, and the reactive part of the solution is usually the most time consuming. Detailed chemical kinetics mechanisms can reach up to tens of thousands species, while numerical simulations of complex reactive flows can handle mechanisms, at most, with a few hundred species. Virtual kinetic mechanisms are a very effective strategy to drastically reduce the computational time spent in the reactive part of numerical simulations. They are formed by artificial species and reaction paths, built from scratch, that are optimized to reproduce the important characteristics of a canonical problem of interest. This work presents the development of a virtual mechanism able to reproduce the temperature evolution and ignition delay times of the thermal ignition of a homogeneous, constant mass, constant pressure, adiabatic, fuel-air mixture. Three different reaction structures are built for a methane-air mixture and their predictions are tested over a range of temperatures from 1000 K to 1500 K and pressures from 1 atm to 3 atm. The limitations observed are due to the small number of reactions and parameters of the kinetic model. But, mechanism reduction methodologies, such as DRG, may present much larger errors if used to achieve the same size of the virtual mechanisms used here.*

Keywords: *virtual chemistry, ignition delay time, reduced kinetic mechanism*

1. INTRODUCTION

The prediction of the chemical kinetics evolution of chemical species is one of the most time consuming operations in reactive flow simulations. Large mechanisms are required to describe with an adequate degree of accuracy the chemical kinetics paths and reactions for large molecules Lu and Law (2009). Although comprehensive mechanisms are needed to build understanding of the chemistry of combustion, their implementation in complex computational models is largely unfeasible. In order to accommodate the state of the art of kinetic mechanisms for large hydrocarbon molecules, e.g., the mechanisms of Naik *et al.* (2011) with 3,500 species and 17,000 reactions and Pei *et al.* (2015) with 2,885 species and 11,754 reactions, several simplification strategies were developed. Such methods can be classified accordingly to the final product and strategy used in schemes that produce skeletal mechanisms, strategies to create analytic mechanisms, and the tabulated strategies. Some of these strategies can also be used in on-the-fly reductions, when the simplification of the mechanism is done simultaneously and in fine tuning with the solution of the transport part of the problem.

Skeletal procedures search and remove unimportant components of the detailed mechanism and therefore reduce its size and complexity. Turányi (1990) published a study in which the importance of species are evaluated by means of removing the reactions where it participates. More recently, graph theory was introduced as a reduction technique by Lu and Law (2005) known as Direct Relation Graph (DRG). Each species is mapped as a node in a directed graph, and the reactions connecting species are mapped as edges. The importance of species in the graph is evaluated and species with negligible effect in the important ones are deemed as redundant and removed. Several studies expanded the basic DRG method, Pepiot-Desjardins and Pitsch (2008) introduced error propagation (DRGEP), and importance index variations, such as the path flux analysis (PFA), proposed by Sun *et al.* (2010). Presently, a large number of variations exist and several authors studied their applicability and efficiency on reducing very large mechanisms, an activity known as Computer Assisted Reduction Mechanism (CARM). Another application of these methods are the on-the-fly reduction schemes, such as the one proposed by Tosatto *et al.* (2011).

The main goal of the analytic methods of reduction is to divide the dynamics of the species transformation into fast and slow domains. Analytic reductions aims at reducing the stiffness of the mechanisms by searching for Quasi Steady State (QSS) candidates to be removed from the system, replacing partial differential by algebraic equations. One of the

basic methods is the Computational Singular Perturbation (CSP), proposed by Lam (1985). One of the main advantages of such strategies is the accuracy and robustness of the final mechanism, since the species are not actually removed, but accounted for through QSS relations.

Tabulated chemistry relies on the fact that the chemical trajectory during a combustion process is in a great extent defined by a smaller sub-space, named a manifold. Such space can therefore be solved in advance, the solution is stored as a table and retrieved during the combustion simulation. The density of the table and the number of inputs needed to retrieve a given information is dictated by the complexity of the problem to be solved.

Despite the reduction techniques have achieved several orders of reduction of complex detailed mechanisms, a limit is always reached, when the accuracy would degenerate at a larger rate than the reduction itself. This limit is intrinsically related to the structure of the detailed mechanism and can hardly be circumvented, even using a combination of strategies.

A strategy proposed by Cailler *et al.* (2017) aims at surpassing this limitation. Contrary to the reduction methodologies that work down from the detailed mechanism, by removing species and reactions as the method advances, the virtual chemistry method builds a virtual mechanism from the ground up, such that the virtual mechanism reproduces the same effects as the detailed mechanism. The final mechanism provided by such methodology can be as accurate as desired, and can predict not only the thermodynamic behavior, but different aspects of the detailed chemistry (Cailler *et al.* (2017); Maio *et al.* (2019); Cailler *et al.* (2020)). Additional information can be added further and then, the final mechanism can be composed only by the necessary or desired modules for the current problem.

This work develops an application of virtual schemes to describe the temperature evolution and the ignition delay time for the thermal ignition of homogeneous, constant mass, constant pressure, adiabatic, fuel-air mixtures. Several strategies and their potential to use as a way to describe Negative Temperature Coefficient (NTC) behavior for complex fuels are evaluated. The methane-air system is used as an example of application.

2. METHODOLOGY

The development of a virtual chemistry requires, at least two steps to be used: Thermodynamic optimization and kinetic optimization. The first step focus on obtaining the optimized coefficients for the constant pressure specific heat function of the n virtual species, generally in the form of NASA-7 polynomials and the virtual species molar mass that better describe the detailed mechanism. The second step optimizes the kinetics parameters for virtual reactions. In addition to the prediction of the adiabatic flame temperature, additional targets and specific reactions can be added to describe different aspects of the combustion, such as pollutant formation or laminar flame speed. The following sections will present the implementations of thermodynamic optimizations and the kinetic optimization targeting thermal ignition, with specifics being discussed as necessary.

2.1 Thermodynamics Optimization

As stated, the virtual chemistry at first must be able to reproduce the thermodynamics properties of the mixture, i.e constant pressure specific heat function and the mixture molar weight. The first is usually implemented in the form of NASA-7 polynomials (Eq. 1 and 2). Therefore, each virtual species in the mechanism requires six coefficients for the NASA-7 polynomial with the addition of one stoichiometric coefficient for every equilibrium condition used.

$$\frac{c_p}{R} = a_1 + a_2 T + a_3 T^2 + a_4 T^3 + a_5 T^4 \tag{1}$$

$$\frac{h}{RT} = a_1 + \frac{a_2}{2} T + \frac{a_3}{3} T^2 + \frac{a_4}{4} T^3 + \frac{a_5}{5} T^4 + \frac{a_6}{T}. \tag{2}$$

Moreover, each species requires the definition of a MW, demanding 7 parameters for each virtual species to be defined. For the thermodynamic part, the fitness function must therefore be able to represent those parameters and was defined as:

$$\epsilon_{thermo} = \sum_{i=1}^{N_c} (\Psi_{det}^{eq}(T, P, \phi)_i - \Psi_{vir}^{eq}(T, P, \phi)_i) \tag{3}$$

where N_c is the number of conditions used, $\Psi_{det}^{eq}(T, P, \phi)_i$ represents the current detailed parameter being optimized, being the equilibrium temperature or the molar weight for the condition i, and $\Psi_{vir}^{eq}(T, P, \phi)_i$ is the virtual counterpart. The Ψ function for the enthalpy is represented as

$$\Psi_i^{eq}(T, P, \phi) = \sum_{s=1}^{N_s} Y_s(T, P, \phi) h_s(T, P, \phi) \tag{4}$$

For the detailed part, all the values are known and thus, this equation become the target for the optimization. For the virtual mechanism, some considerations can be done: there are some species that does not requires the optimization, such as the fuel, oxidizer and diluent as they can have the same properties of the detailed species. By doing this, the fitness calculation can be improved by removing the contribution of those species from the Ψ, which makes sure that the virtual species are optimized to match the properties of the burned composition. Therefore, we can rewrite the fitness function as

$$\epsilon_{thermo} = \sum_{i=1}^{N_c} \sum_{l=1}^{N_{thermo}} (\bar{a}_l^{vir}(T,P,\phi)_i - \delta_l^{det}(T,P,\phi)_i) \tag{5}$$

$$\delta_l^{det}(T,P,\phi)_i = \bar{a}_l^{det}(T,P,\phi)_i - \bar{a}_{l,A}^{det}(T,P,\phi)_i \tag{6}$$

$$\bar{a}_l^{vir}(T,P,\phi)_i) = \sum_{k=1}^{N_{vir}} a_{l,k}^{vir} \alpha_k^{vir} Y_P^{det}(T,P,\phi)_i \tag{7}$$

Where N_{thermo} is the number of thermodynamics coefficients, α_k^{vir} is the stoichiometric coefficient for the k virtual species, $a_{l,k}^{vir}$ is the thermodynamic parameter l of the virtual species k, A is the group of species which have identical counterparts in both, detailed and virtual schemes (fuel, oxidizer and diluent) and P represent all detailed species not include in A. The fitness function present yet another unknown variable, the stoichiometric coefficient for the virtual species. The direct inclusion of these coefficients in the optimization scheme requires a new set of $N_c \times (N_{vir} - 1)$ parameters to be optimized. To ease the problem, Cailler *et al.* (2017) further divided the problem in two parts, the first part consider that for every group of N_{vir} there is a subset of m coefficients that perfectly describe the detailed mechanism and can be expressed as

$$\begin{cases} \sum_{k=1}^{N_{vir}} a_{1,k}^{vir} \alpha_k^{vir} Y_P^{detd}(T,P,\phi)_i = \delta_1^{det}(T,P,\phi)_i & \text{(8a)} \\ \dots & \text{(8b)} \\ \sum_{k=1}^{N_{vir}} a_{m,k}^{vir} \alpha_k^{vir} Y_P^{det}(T,P,\phi)_i = \delta_m^{det}(T,P,\phi)_i & \text{(8c)} \end{cases}$$

If an additional consideration of $\sum_{k=1}^{N_{vir}} \alpha_k^{vir} = 1$ is made, we can rewrite the equations as

$$\begin{cases} \sum_{k=1}^{N_{vir}-1} \left[a_{1,k}^{vir} \alpha_k^{vir}\right] + a_{1,N_{vir}}^{vir} \left(1 - \sum_{k=1}^{N_{vir}-1} \alpha_k^{vir}(T,P,\phi)_i\right) = \frac{\delta_1^{det}}{Y_P^{det}}(T,P,\phi)_i & \text{(9a)} \\ \dots & \text{(9b)} \\ \sum_{k=1}^{N_{vir}-1} \left[a_{m,k}^{vir} \alpha_k^{vir}\right] + a_{m,N_{vir}}^{vir} \left(1 - \sum_{k=1}^{N_{vir}-1} \alpha_k^{vir}(T,P,\phi)_i\right) = \frac{\delta_m^{det}}{Y_P^{det}}(T,P,\phi)_i & \text{(9c)} \end{cases}$$

If $m = N_{vir} - 1$, the system present $N_{vir} - 1$ equations and unknown variables α_k^{vir}, and with a given set of thermodynamic coefficients $a_{m,k}^{vir}$, the system can be used to calculate the corresponding stoichiometric α_k^{vir}. Therefore, the first step for the thermodynamics optimization can be modified and the new fitness calculation takes the form

$$\epsilon_{thermo,1} = \sum_{i=1}^{N_c} \sum_{k=1}^{N_{vir}} v_k \tag{10}$$

$$v_k = \begin{cases} 0 & \text{if } 0 < \alpha_k^{vir} < 1 \\ 1 & \text{otherwise} \end{cases} \tag{11}$$

where α_k^{vir} are obtained from the solution of the system. This first optimization stop when $\epsilon_{thermo,1}$ reaches zero. The second part of the optimization target the last $N_{vir} - m$ parameters, using the following equation

$$\epsilon_{thermo,2} = \sum_{i=1}^{N_c} \sum_{l=m}^{N_{thermo}} (\bar{a}_l^{vir}(T,P,\phi)_i - \delta_l^{det}(T,P,\phi)_i) \tag{12}$$

And finally the molar weight optimization, equation 3 is used, with a the Ψ function being the mixture molar weight.

2.2 Kinetics Optimization

Ignition delay time and the temperature transient profile are the main targets of this study. The model used is a homogeneous, constant mass, constant pressure, adiabatic reactor (Eq. 13 and 14) and IDT was defined as the point where the temperature increases by 400 K.

$$\frac{dT}{dt} = -\frac{c_p}{\rho}\sum_k h_k \dot{\omega}_k \tag{13}$$

$$\frac{dY_k}{dt} = \frac{MW_k}{\rho}\dot{\omega}_k \tag{14}$$

Here, $\dot{\omega}_k$ is the net production rates for species k. The set of equations are solved using the SCIPY package (Virtanen *et al.* (2020)) while an in-house code handles the chemistry part. Virtual reactions are modeled following the elementary reaction structure. The rate constant of each reaction is modeled by an Arrhenius form (Eq. 15), therefore each reaction requires at least two parameters, the pre-exponential factor A and the activation energy E_a, and in the later cases, the temperature exponent b is also used. Aside from these parameters, the order of each reactant (see Eq. 16 for the rate of progress) was also optimized.

$$k_r = AT^b exp(-E_a/RT) \tag{15}$$

$$q_r = k_r \prod_{r=0}^{n_{reactants}} [r]^{\alpha_r} \tag{16}$$

Additional intermediate species may also be used, which requires another set of NASA-7 parameters to be optimized. These new species are not considered in the thermodynamics optimization step as they are not desired to exists at the equilibrium state, therefore its NASA-7 coefficients are optimized with the kinetic parameters. To ease the optimization process, only the first five coefficients are optimized, being the sixth obtained from Eq. 17 as follows

$$a_6 = \frac{\Delta H_v}{R} - \left(a_1 T_0 + \frac{a_2}{2}T_0^2 + \frac{a_3}{3}T_0^3 + \frac{a_4}{4}T_0^4 + \frac{a_5}{5}T_0^5\right) \tag{17}$$

where ΔH_v is set to be the enthalpy of formation for the virtual species at 298K. Also, a penalizing factor is added to the fitness calculations to ensure that all the intermediaries are consumed at the end of ignition.

The objective function has two components. The first is directly defined as the relative error between the IDT predictions with the virtual scheme and with the detailed mechanism as

$$u_{idt}^j = \frac{|\tau_d^j - \tau_v^j|}{min(\tau_d^j, \tau_v^j)} \tag{18}$$

where τ refers to the IDT and the subscripts d and v are used for detailed and virtual mechanisms respectively while j represent the condition. The minimum in the denominator is used to discourage the genetic optimization to be trapped in very fast ignition cases.

The second component is calculated from the error between the temperature profiles over a time domain normalized by the IDT (Eq. 19), to ensure that the shape of the temperature curve is taken into account separated from the effect of the IDT. This methodology helps to adjust of the time domain used for the optimization by using a normalization space and all the error integrals presented in Eq. 20 are performed between $0 <= t_{n,i}^j <= 1.5$, which encompass all the ignition up to a burnt state.

$$t_{n,i}^j = \frac{t_i}{\tau_j} \tag{19}$$

$$u_T^j = \sqrt{\int_{t_n=0}^{1.5} \left(\frac{T^v(t_n) - T^d(t_n)}{T^d(t_n)}\right)^2 dt} \tag{20}$$

The fitness calculation for each condition is calculated by Eq. 21, which couple both errors. The objective function is them defined as Eq. 22 using a mean square average and the optimization targets become the minimization of this function.

$$\epsilon_k^j = (1 + u_{idt}^j)(1 + u_T^j) - 1 \tag{21}$$

$$\epsilon_k = \frac{1}{n_{cond}} \sqrt{\sum_{j=1}^{n_{cond}} (\epsilon_k^j)^2} \tag{22}$$

Additional weight parameters can still be used, mainly to help improve the IDT predictions however are not necessary as the improvements were to small to be accounted for.

2.3 Optimization Algorithm

Genetic optimization algorithms are used in this study and are implemented in an in-house python algorithm, using CANTERA (Goodwin *et al.* (2017)) to handle thermodynamics and kinetics calculations for the detailed mechanisms and the SCIPY package (Virtanen *et al.* (2020)) for the differential equations solver. The choice of such optimization methodology is mostly due to the complexity of the problem, as an initial point to be start is not easily defined and the fitness function is not smooth with several local optima regions with additional points of solver problems and non-ignition cases, which are not easily treated by other methods.

2.4 Optimization Setup

As discussed and presented in the Thermodynamics Optimization section, a set of stoichiometric coefficients are calculated for each unburned condition and due to the large amount and higher temperature cases, significant variations on the stoichiometric coefficients can appear. this variation does not lead to great problems when low temperature cases are used but may prove a issue on the higher cases. Figure 1 shows the adiabatic temperature for the methane, from the initial Temperature of 300 K (the lowest curve) up to 1500 K. It's easy to observe the difference on the curves, mainly at the ϕ limits. That difference in the behavior in conjunction with the aforementioned variations on the stoichiometric coefficients and the higher order of the NASA polynomials highly impact the optimization.

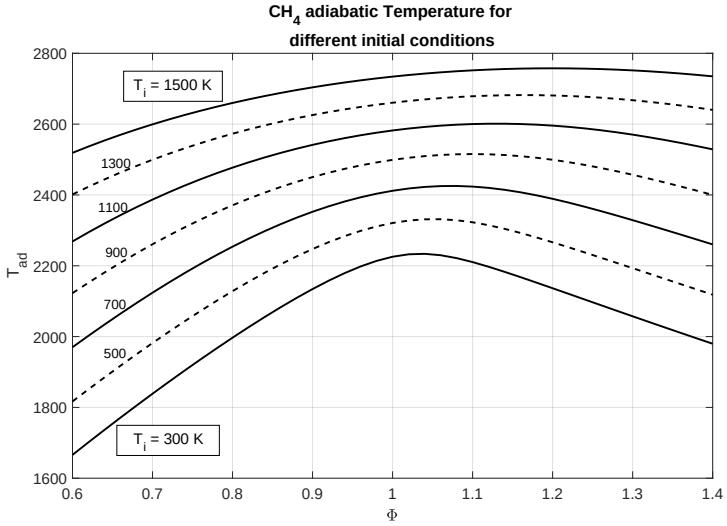

Figure 1: CH_4 Adiabatic temperatures for various ϕ and T_i from 300 K to 1500 K

To minimize such problems, the temperature range was restrain between 1000 K and 1500 K, and only one set of stoichiometric coefficients were used. The set of stoichiometric coefficient for the $\phi = 1.0$ and $T_i = 1000K$ was used to optimize the second step of the thermodynamics optimizations. The purpose of such simplifications was to first, produce the best set of stoichiometric that could represent all the conditions and second, use no correction function for the products values in the virtual reactions. Such implementation brings benefits for the kinetic implementation, however the burned temperature prediction suffer additional errors.

The method was applied to a methane-air mixture, using the GRI-Mech 3.0 (Smith *et al.* (2018)) as the detailed mechanism. The thermodynamic optimization was done at three temperatures (1000 K, 1300 K and 1500 K), two pressures (1 atm and 3 atm) and several equivalence ratios (from 0.8 to 1.2). For the kinetic optimization, the same conditions were used except the equivalence ratio, which was kept at stoichiometry. Three cases of virtual mechanisms are optimized and are summarized in Table 1.

Table 1: Summary of kinetic models.

Name	Mechanism	No. of reactions	No.of intermediaries	No. of kinetic Parameters
One RXN	$\nu_F F + \nu_{Ox} O \rightarrow \sum_{i=0}^{n_v} \nu_i V_i$	1	-	4
One INTER	$\nu_F F + \nu_{Ox} O \rightarrow I$ $I \rightarrow \sum_{i=0}^{n_v} \nu_i V_i$	2	1	13
Two INTER	$\nu_F F + \nu_{Ox} O \rightarrow I_1$ $I_1 \rightarrow \sum_{i=0}^{n_v} \nu_i V_i$ $\nu_F F + \nu_{Ox} O \rightarrow I_2$ $I_2 \rightarrow \sum_{i=0}^{n_v} \nu_i V_i$	4	2	24

Model One RXN is a basic one-step global reaction model with n_v products. Model One INTER uses a set of two sequential reactions with one intermediate. Model Two INTER uses a set of two parallel paths of two sequential reactions involving two different intermediates. The number of kinetics parameters to be optimized grows with the number of reactions and intermediaries. A virtual chemistry was optimized until a set amount of generations without improvements are achieved, ensuring all the mechanisms uses the same stop criteria.

3. RESULTS AND DISCUSSIONS

The optimization of the kinetics follows, using the IDT and the temperature profile as targets. The three kinetics models, identified in Table 1, were used. Figure 2 presents the predictions of IDT from the three virtual mechanisms at two pressure levels and temperatures, with T_u from 1000 K up to 1500 K. All virtual mechanism present an apparent good agreement with the predictions of the detailed model.

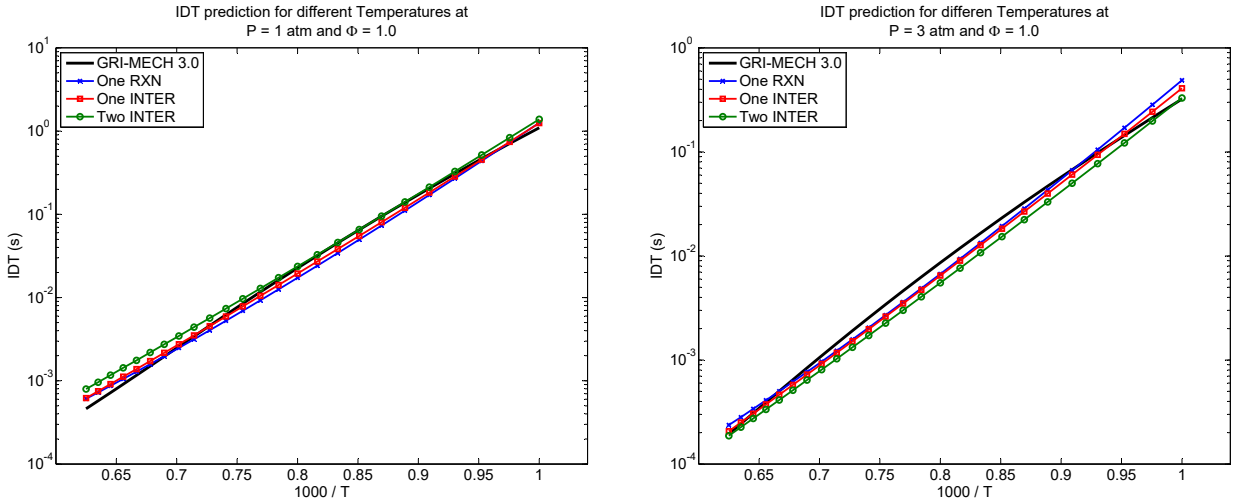

(a) 1 atm (b) 3 atm

Figure 2: Comparison of IDT calculated with the virtual and detailed mechanisms.

Figures 3 and 4 presents the relative errors between the predictions by the virtual and the detailed mechanisms. Now, we realize that errors greater than 50% are observed at the lower temperatures. The model with one intermediate presents the best compromise overall. All the virtual mechanisms predicted the IDT with a very similar behavior indicating that the small number of reactions and parameters used is not enough to properly model autoignition problems. A more accurate prediction of the IDT could be achieved by using a greater weight for the IDT part of the kinetic fitness function.

Figures 5 and 6 presents the prediction of the transient temperature profiles at initial conditions of 1000 K and 1 atm and 1500 K and 3 atm respectively, which correspond to the slowest and fastest ignitions times used for this study. The difference on the burned temperature described in the beginning of this section can be better observed in 5. The predictions for other conditions follow the same trends and are not showed here. The closest prediction of the overall temperature profile is provided by the two intermediates model, followed by the one intermediary although the One RXN has a better prediction on the lower Temperature case .

The additional parameter b of the Arrhenius equation was used to test the virtual mechanism capability. In the IDT

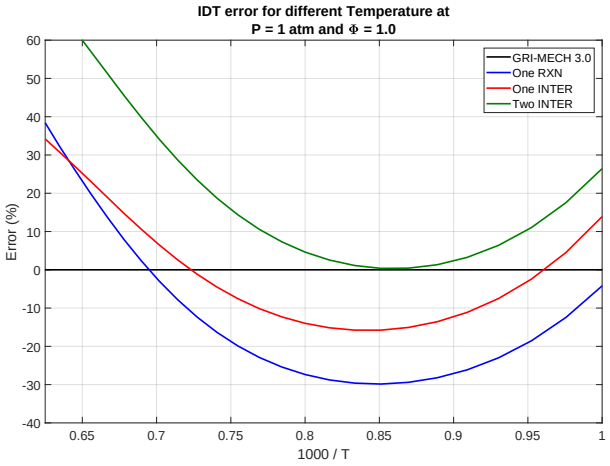

Figure 3: Relative error of IDT at 1 atm.

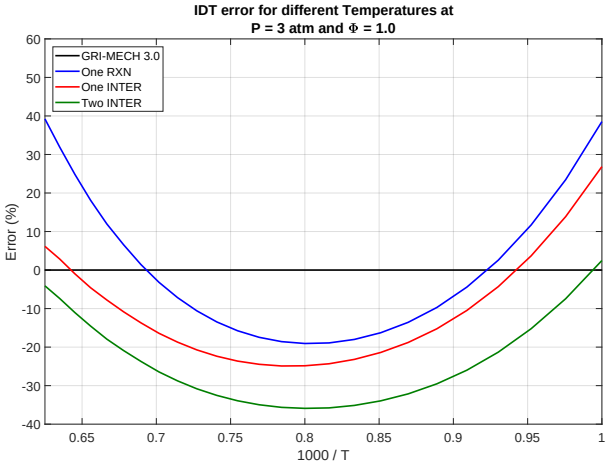

Figure 4: Relative error of IDT at 3 atm.

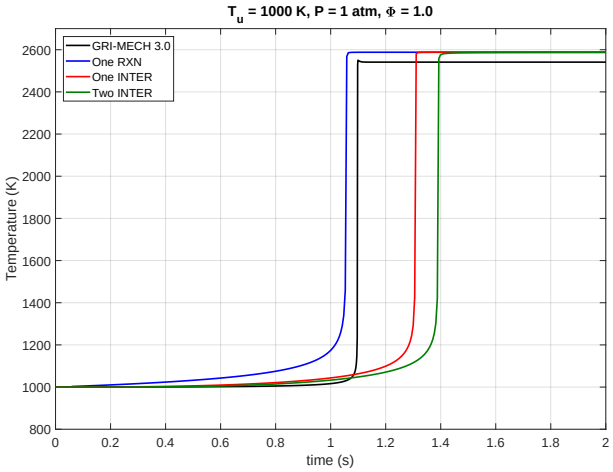

Figure 5: T_u = 1000 K and P = 1 atm.

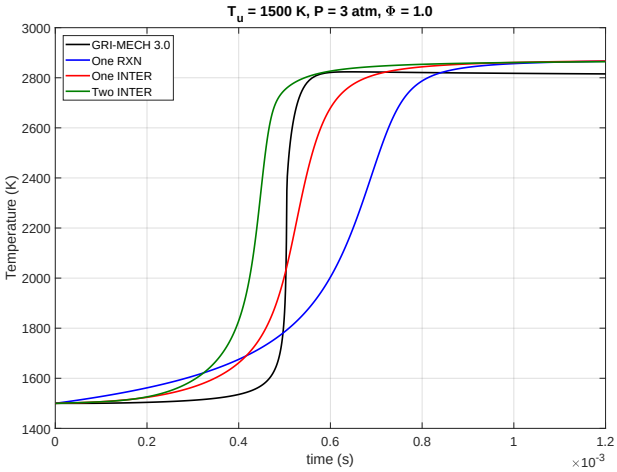

Figure 6: T_u = 1500 K and P = 3 atm.

prediction, little to no improvement was achieved and the same discussion can be applied here, therefore, no figures were shown here showing IDT predictions. The major improvements were the temperature profiles, as can be observed in Figures 7 and 8. The cases presented here are the T_u of 1500 K and 3 atm, as the effects of the parameters are easily observed. Figure 7 shows the comparison between the mechanisms and the detailed profile while Fig. 8 presents a comparison between the cases with and without the b parameter. The great improvement here is the faster temperature rise after the ignition, as observed in the One reaction and one intermediary cases.

The same effect is observed at other conditions with reduced effect as the ignition is slower. One of the drawbacks of using the exponential coefficient into the optimization is the fact that its effect is similar to the combined results obtained with the pre-exponential coefficient (A) and the Energy of Activation (E_a), i.e. represent an exponential parameter based on the temperature. To mitigate this the optimization of b is performed with an already optimized mechanism.

The time spent in the use of the mechanisms developed here in numerical simulations is much smaller than the computational time for the detailed mechanism. To evaluate the computational time of the virtual mechanism, an Intel Core i7-7700HQ, 2.8 GHz was used and the average reduction of the computational time was one order of magnitude, and at the worst case, a 50% reduction. There was no significant changes when using the b coefficient. Here is important to note that improvements on the computational time are still possible as the virtual scheme was not used in an optimized code.

The methodology developed here could also be used combined with the prediction of flame speed, such as in Cailler *et al.* (2017), Maio *et al.* (2019) and Cailler *et al.* (2020), in order to develop a more comprehensive virtual mechanism. Besides, although the optimizations used methane as the fuel, this scheme can be applied to other fuels. However, the behavior of virtual mechanisms for a fuel that presents NTC has not been tested yet.

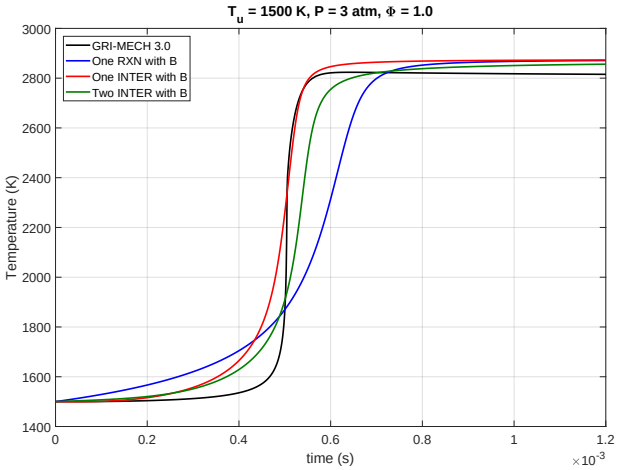

Figure 7: T_u = 1500 K and P = 3 atm.

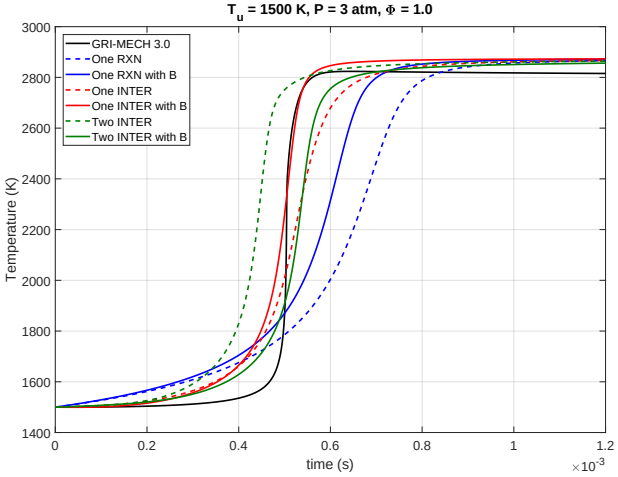

Figure 8: Comparison between using One and Two INTER cases when using the additional B parameter in the optimization.

4. CONCLUSIONS

A virtual chemistry model was implemented and optimized for IDT problems. The limitations of the virtual mechanisms at this point are related to the small number of reactions and possibly also to the small number of parameters used to model the rate constant. However, mechanism reduction methodologies, such as DRG, may present much larger errors if used to achieve the same size of the virtual mechanisms used here. Although the relative error could be reach the 50% mark, is important to note the great variations on experimental results and different detailed kinetic mechanism.

5. ACKNOWLEDGEMENTS

This work was supported by the Brazilian National Council for Scientific and Technological Development (CNPq).

6. REFERENCES

Cailler, M., Darabiha, N. and Fiorina, B., 2020. "Development of a virtual optimized chemistry method. application to hydrocarbon/air combustion". *Combustion and Flame*, Vol. 211, pp. 281–302. doi: https://doi.org/10.1016/j.combustflame.2019.09.013.

Cailler, M., Darabiha, N., Veynante, D. and Fiorina, B., 2017. "Building-up virtual optimized mechanism for flame modeling". *Proceedings of the COmbustion Institute*, Vol. 36, pp. 1251–1258. doi: http://dx.doi.org/10.1016/j.proci.2016.05.028.

Goodwin, D.G., Moffat, H.K. and Speth, R.L., 2017. "Cantera: An object-oriented software toolkit for chemical kinetics, thermodynamics, and transport processes". `http://www.cantera.org`. doi:10.5281/zenodo.170284. Version 2.3.0.

Lam, S.H., 1985. "Singular perturbation for stiff equations using numerical methods". *Recent Advances in the Aerospace Sciences*, pp. 3–19.

Lu, T. and Law, C.K., 2005. "A directed relation graph method for mechanism reduction". *Proceedings of the Combustion Institute*, Vol. 30, No. 1, pp. 1333–1341. doi:10.1016/j.proci.2004.08.145.

Lu, T. and Law, C.K., 2009. "Toward accomodating realistic fuel chemistry in large-scale computations". *Progress in Energy and Combustion Science*, Vol. 35, pp. 192–215. doi:10.1016/j.pecs.2008.10.002.

Maio, G., Cailler, M., Mercier, R. and Fiorina, B., 2019. "Virtual chemistry for temperature and co prediction in les of non-adiabatic turbulent flames". *Proceedings of the COmbustion Institute*, Vol. 37, pp. 2591–2599. doi: https://doi.org/10.1016/j.proci.2018.06.131.

Naik, C.V., Westbrook, C.K., Herbinet, O., Pitz, W.J. and Mehl, M., 2011. "Detailed chemical kinetic reaction mechanism for biodiesel components methyl stearate and methyl oleate". *Proceedings of the Combustion Institute*, Vol. 33, pp. 383–389. doi:10.1016/j.proci.2010.05.007.

Pei, Y., Mehl, M., Liu, W., Lu, T., Pitz, W.J. and Som, S., 2015. "A multi-component blend as a diesel fuel surrogate for compression ignition engine applications". *Journal of Engineering for Gas Turbines and Power*, Vol. 137, No. 11. doi:10.1115/1.4030416.

Pepiot-Desjardins, P. and Pitsch, H., 2008. "An efficient error-propagation-based reduction method for large chemical kinetic mechanisms". *Combustion and Flame*, Vol. 154, pp. 67–81. doi:10.1016/j.combustflame.2007.10.020.

Smith, G.P., Golden, D.M., Frenklach, M., Moriarty, N.W., Eiteneer, B., Goldenberg, M., Bowman, C.T., Hanson, R.K., Song, S., Gardiner, W.C.J., Lissianski, V.V. and Qin, Z., 2018. "Gri-mech 3.0". `http://www.me.berkeley.edu/gri_mech/`.

Sun, W., Chen, Z., Gou, X. and Ju, Y., 2010. "A path flux analysis method for the reduction of detailed chemical kinetic mechanisms". *Combustion and Flame*, Vol. 157, pp. 1298–1307.

Tosatto, L., Bennett, B.A.V. and Smooke, M.D., 2011. "A transport-flux-based directed relation graph method for the spatially inhomogeneous instantaneous reduction of chemical kinetic mechanisms". *Combustion and Flame*, Vol. 158, pp. 820–835. DOI:10.1016/j.combustflame.2011.01.018.

Turányi, T., 1990. "Reduction of large reaction mechanisms". *New Journal of Chemistry*, Vol. 14, pp. 795–803. doi: 0398-9836/90/11 795 9.

Virtanen, P., Gommers, R., Oliphant, T.E., Haberland, M., Reddy, T., Cournapeau, D., Burovski, E., Peterson, P., Weckesser, W., Bright, J., van der Walt, S.J., Brett, M., Wilson, J., Jarrod Millman, K., Mayorov, N., Nelson, A.R.J., Jones, E., Kern, R., Larson, E., Carey, C., Polat, İ., Feng, Y., Moore, E.W., Vand erPlas, J., Laxalde, D., Perktold, J., Cimrman, R., Henriksen, I., Quintero, E.A., Harris, C.R., Archibald, A.M., Ribeiro, A.H., Pedregosa, F., van Mulbregt, P. and Contributors, S..., 2020. "SciPy 1.0: Fundamental Algorithms for Scientific Computing in Python". *Nature Methods*, Vol. 17, pp. 261–272. doi:https://doi.org/10.1038/s41592-019-0686-2.

7. RESPONSIBILITY NOTICE

The authors are solely responsible for the printed material included in this paper.